REPORT DOCUMENTATION PAGE

Form Approved
OMB NO. 0704-0188

1. AGENCY USE ONLY (Leave Blank)	2. REPORT DATE January 2000	3. REPORT TYPE AND DATES COVERED Final Report

4. TITLE AND SUBTITLE
Semiconductor Composites for Thermoelectric Applications

5. FUNDING NUMBERS
DAAG55-98-1-0527

6. AUTHOR(S)
Tito Ernesto Huber

7. PERFORMING ORGANIZATION NAME(S) AND ADDRESS(ES)
Howard University
Washington, DC 20059

8. PERFORMING ORGANIZATION REPORT NUMBER

9. SPONSORING / MONITORING AGENCY NAME(S) AND ADDRESS(ES)
U. S. Army Research Office
P.O. Box 12211
Research Triangle Park, NC 27709-2211

10. SPONSORING / MONITORING AGENCY REPORT NUMBER
ARO 39088.3-MS

11. SUPPLEMENTARY NOTES
The views, opinions and/or findings contained in this report are those of the author(s) and should not be construed as an official Department of the Army position, policy or decision, unless so designated by other documentation.

12 a. DISTRIBUTION / AVAILABILITY STATEMENT	12 b. DISTRIBUTION CODE
Approved for public release; distribution unlimited.	

13. ABSTRACT (Maximum 200 words)

The design of composite materials consisting of a mixture of conducting and insulating phases in the nanometer scale is actively being investigated because of their potential applications to microelectronics and photonic technologies. We have developed a high-pressure, high-temperature injection technique for the synthesis of composites using nanochannel glass as template structure. In this way we have prepared high density semiconductor nanowire arrays and networks from porous matrices. Using this technique we have prepared wire arrays that we have used in a number of experiments designed to prove the electrical transport properties. We report here work on the electromagnetic field propagation in wire arrays, thermoelectric properties of Bi and bismuth tellunde wire array composites and the electronic transport in Bi nanowire networks.

14. SUBJECT TERMS

15. NUMBER OF PAGES

16. PRICE CODE

17. SECURITY CLASSIFICATION OR REPORT	18. SECURITY CLASSIFICATION ON THIS PAGE	19. SECURITY CLASSIFICATION OF ABSTRACT	20. LIMITATION OF ABSTRACT
UNCLASSIFIED	UNCLASSIFIED	UNCLASSIFIED	UL

Final Report of Grant DAAG55-98-1-0527

Semiconductor Composites for Thermoelectric Applications

1 Microporous Template Injection

The template injection technique allows for the synthesis of conductor-insulator nanocomposites for both optical and electrical performance. Composites with highly reproducible properties are obtained in this way, since the injected material "copies", to a large extent, the channel structure of the matrix. For the various metals and semiconductors we have investigated, we have found that an externally applied isostatic pressure is needed to overcome surface tension effects which prevent the melt from entering the narrow channels of insulating hosts. An estimate for the diameter d of the smallest channel filled at pressure P can be obtained from the Washburn equation:

$$d = -4\gamma\cos\alpha / P \qquad (1)$$

where γ is the surface tension of the liquid and α is the contact angle between the liquid and the insulator ($\alpha > 90^\circ$ for non-wetting liquids). Values for the surface tension of some liquid metals and semiconductors of interest span the 100-600 dyne/cm range. Using a mid-range surface tension of 300 dyne/cm and assuming the least favorable case of complete non-wetting ($\alpha = 180^\circ$), the Washburn equation becomes $d = 12$ nm / P, where P is measured in kilobars. Then, for a modest pressure of, for example, 4 kbar all channels larger than 3 nm in diameter will be filled with the impregnant.

Most of the nanocomposites have been prepared with an injection apparatus we have designed and built ourselves. It is based on a high pressure pump using fluids as pressure transmission medium, and on an externally heated reactor with a maximum operating pressure of 4 kbar at 800 °C. The

reactor and injection assembly are schematically illustrated in Figure 1.

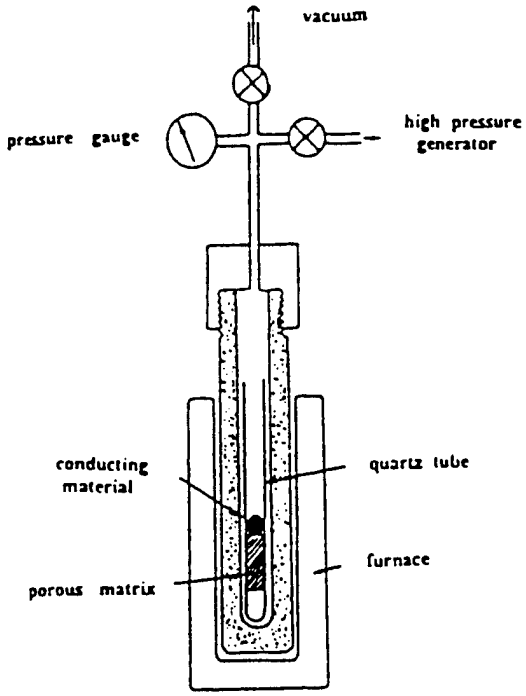

Figure 1: Injection reactor

Details about the apparatus construction and operation have been reported previously.[10] Briefly, the reactor is heated in vacuum to a temperature above the metal (or semiconductor) melting point. The metal melts and surrounds the porous matrix making a tight seal. A pressure-transmitting fluid is then introduced and its pressure gradually raised, the molten metal is then pushed into the matrix channels by the isostatic pressure. When the injection is complete the reactor is cooled and the metal solidifies inside the channels, the high pressure is then removed. Using water or oil as pressure-transmitting fluid may cause oxidation or contamination. In such case, the porous matrix and metal are initially packed in an evacuated, thin-wall, sealed metal capsule which collapses under the high pressure. We have prepared composite samples of typical dimensions of 1 cm. From gravimetric measurements performed on numerous samples we have determined that the impregnant fills 92-97% of the pore volume for the smallest, nanometer-size channels.

A fundamental limit of the high temperature injection process is established by the sintering of the template which takes place at these temperatures. Figure 2 shows how the porosity decreases with temperature for two templates we have used: porous silica (6 nm average pore size, interconnected

pores)[11] and nanochannel alumina (parallel channels, 200 nm in diameter)[12]. For these templates, the choice of impregnant is limited to materials with a melting point below 1,000 °C.

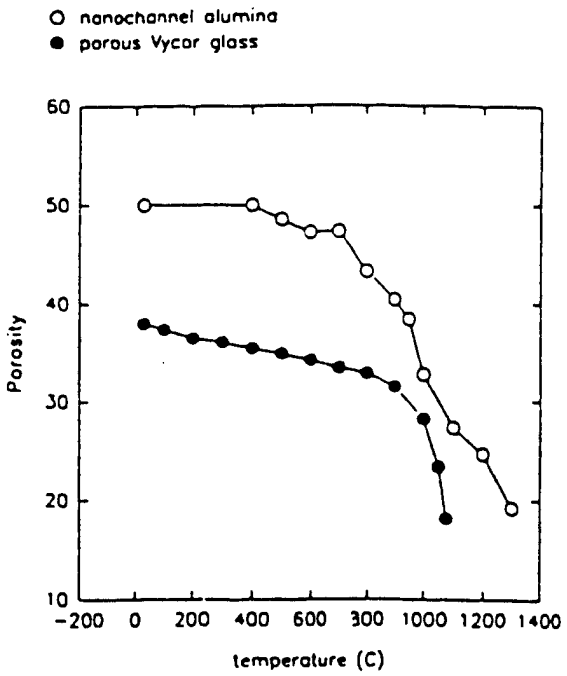

Figure 2: Template sintering.

2 Electromagnetic Field Propagation in Wire Array Composites

Recent progress in the design of 3-dimensional micro- and nanostructured materials holds the promise of novel electromagnetic field (EMF) response. Inhibited spontaneous emission[13] and extremely low frequency plasmon (ELFP)[14] are two aspects of this behavior that have received attention recently. Electronic mesoscopic[15] and quantum confinement effects further enrich this field. In condensed matter, reduced dimensionality often leads to unique behavior and that is the case of the one-dimensional "artificial dielectric" consisting of an array of parallel wires embedded in an insulator. This composite has the distinction of being simultaneously optically transmissive and electrically conductive along the wire length. According the effective medium models, high optical transmittance can be achieved when the metal wires are isolated from each other in the direction of the photon electric field. The field can then induce a self-screening depolarization charge on the surface of the metal structures which prevents it from penetrating further into the metal. Elastic scattering is inhibited

if the composite building unit and spatial periodicity are smaller than the wavelength of light. Conductivity is not impaired as long as the electron mean free path is much smaller than the wire diameter. Aspnes, Heller and Porter[16] studied theoretically the problem of conductive structured metallic films. Metal films of thickness greater than several hundred angstroms are optically opaque and the prospect of designing metal-insulator composites to be conductive while retaining optical transparency over micron-length scales is exciting. Also, this leads to a variety of possible applications in optoelectronic and photoelectrochemical technologies.

It is well established that wire grids are efficient polarizers and they have high transmission even for separation $s<<\lambda$. Brandili and Sievers's[17] experiments on the propagation of far-infrared in stacks of parallel-plate waveguides exploited this phenomenon for the study of the electromagnetic response of superconductors in the far-infrared. The optical properties of wire arrays have been addressed before but the materials available were not well suited for this research. Heller, Aspnes, Porter, Sheng, and Vadimsky[18] have experimented with photoelectrochemically deposited Pt metal films. Because of the structural complexity, the films utilized are composed of small particles assembled in three levels of structure, and since the films are only partially conductive, the experiment is not conclusive. M.J. Tierney and C.R. Martin[19] have considered arrays of cylinders of diameter d small relative to the wavelength of light and of length l comparable to such wavelength. The metal particles were prepared by electrochemical deposition into the channels of a mesoporous membrane. In those experiments the cylinders are too short and their relative position is not well controlled. Recently, Foss, Hornyak, Stockert, and Martin[20] have studied arrays of gold cylinders of controlled radius and aspect ratio. Cylinders of diameter between 30 and 60 nm and length $l < 800$ nm were prepared. Although the optical absorption of such system follows qualitatively the Maxwell-Garnett model predictions, the system does not lend itself to a simple description at short wavelengths where the cylinder radius $a \leq \lambda$. The authors introduce a phenomenologic modification of MG to account for dynamic depolarization effects. Aside from the fact that the conductivity of those arrays has not been demonstrated, the length of the cylinders, as well as their relative position within the membrane channels, has a considerable degree of randomness and a more clearly defined sample geometry is needed.

In a recent publication we have examined the far-infrared transmission of thick (90 μm) densely packed arrays of 5-μm radius In wires.[21] (Fig. 3). The measured absorption (Fig. 4) increases as $k^{0.45\pm0.07}$ and can be explained by considering electromagnetic energy losses through dissipation by eddy currents. This magnetic dipole effect has been treated phenomenologically by calculating the eddy

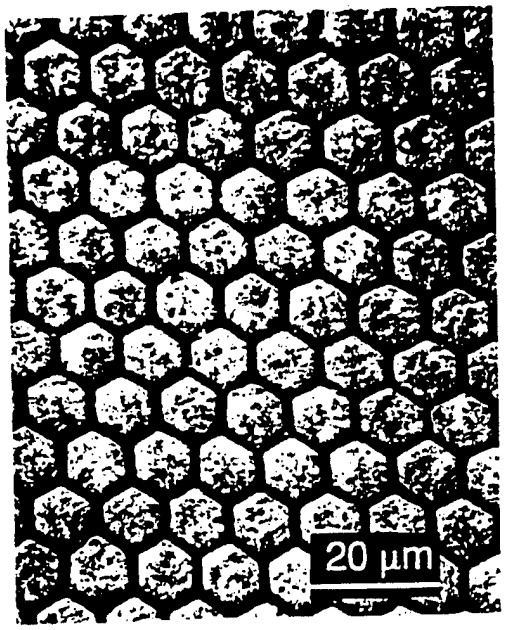

Fig. 3. Electron micrograph of an indium microwire array (top view).

currents dissipation in the quasistatic approximation. The resulting optical absorption is $\alpha_{MD}=2\pi^2 n_g (v_m/a) (c/\sigma)^{1/2} k^{1/2}$, where n_g is the insulator index of refraction, v_m in the metal volume fraction, a is the wire radius, σ is the wire conductivity and c is the velocity of light in vacuum. The frequency dependence predicted, $k^{1/2}$, is indistinguishable from the experimental frequency dependence in the range investigated, which is $k^{0.47\pm0.07}$ (Fig. 4). However, the experimental data indicate an effective surface conductivity σ_{eff} of 1.4×10^{15} sec^{-1}. This is a factor of 80 smaller than σ_B, the bulk conductivity. This in not surprising since actual eddy current losses in microwave resonators are always in excess to those calculated from bulk parameters due to surface roughness, oxide layer, and anomalous skin depth effects. An important dynamical effect of eddy currents is the magnetic field exclusion from the wire interior as the skin depth $\delta << d$. This effectively shields the wire interior from the EMF thereby decreasing the calculated absorption. This diamagnetism has been treated by assigning the medium an effective magnetic permeability μ that is less than 1. In Ref. 22 we present a self-consistent calculation of the effective medium dielectric and diamagnetic properties of metal-insulator composites. The electromagnetic field distribution is illustrated in Fig. 5.

The absorption exhibits an additional k^2 dependence due to losses in the glass matrix at higher frequencies in the mid-infrared. We find that the reflectivity is low, in comparison to the bulk metal, and that the velocity of propagation of electromagnetic fields (EMF) is given by c/n_i, where n_i is the insulator dielectric constant. Further experimental results of propagation of microwave radiation through such composites show good agreement with this theory.[23]

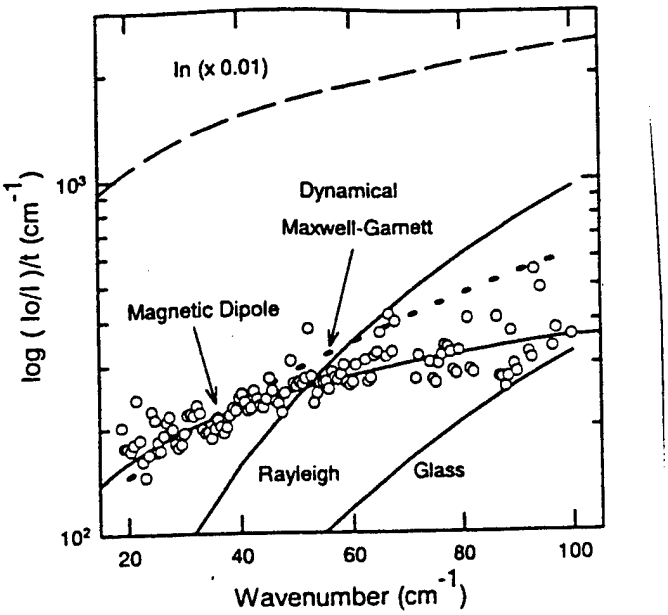

Fig. 4. Far-infrared absorbance of the 10-micron diameter In wire array composite (open circles). Unpolarized light impinges parallel to the channels, that is, to the wire length. The results of the calculations are shown as solid lines. The absorbance of a (thick) film of indium is also shown (dotted line).

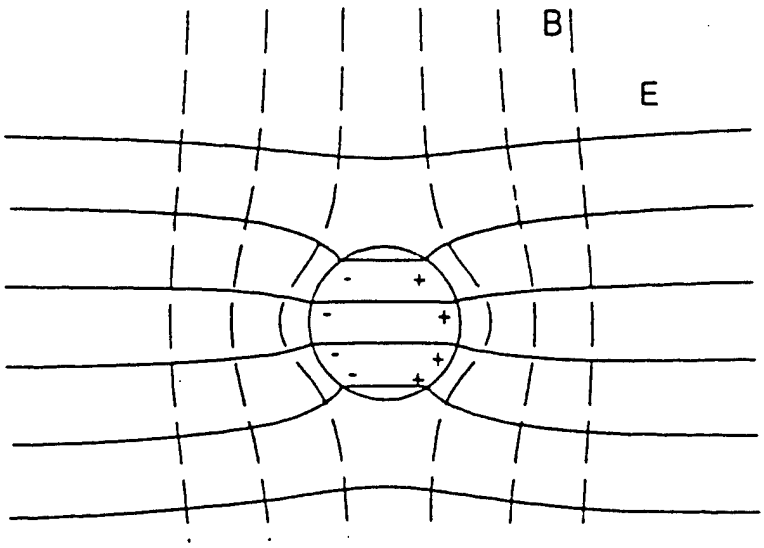

Fig. 5. Electric and magnetic field distribution around a wire

The topic of artificial dielectrics is well known in the general field of dielectric structures.[24,25] The idea of artificial dielectrics is to microengineer an enlargement of the index of refraction $\eta = (\varepsilon\mu)^{1/2}$. The case considered here, where EM modes propagate parallel to the wire length in our wire arrays is not suitable for that application because dielectric constant and magnetic permeability effects tend to compensate mutually. On a related matter, we have applied our expression for the dielectric constant to empty capillary arrays. It turns out that this structure has a very low dielectric constant and this is important for microelectronics manufacturing.[26]

3 Thermoelectric properties of Bi and Bi_2Te_3 wire composites

The area of thermoelectrics is one of opportunity for technical innovation. Thermoelectric cooler and generator performance has stagnated for the past thirty years or so. An important factor limiting this technology has been the availability of appropriate thermoelectric materials. The suitability of a material for thermoelectric cooling applications is defined by the thermoelectric figure of merit $Z = S^2 \sigma/\kappa$, where S is the Seebeck coefficient, σ is the conductivity, and κ is the thermal conductivity.[27] Efforts to increase Z in conventional, bulk materials have been hampered by the interrelation between the three parameters which results in an adverse effect on the other two parameters when improvement of one of them is attempted. Currently, the materials with the highest figure of merit at room temperature are bismuth telluride and related ternary alloys such as $Bi_2Te_{2.7}Se_{0.3}$ and $Bi_{0.5}Sb_{1.5}Te_3$, where the thermoelectric figure of merit ZT peaks at around 0.96.[28] At low temperatures, in the range between 77 K and 200 K, $Bi_{1-x}Sb_x$ with $x \sim 0.1$ has a thermoelectric figure of merit that peaks at around 0.2. A closely related property, the thermomagnetic figure of merit Z_MT, which measures the cooling and heating efficiency of a given material when aided by an external magnetic field, is 0.5 for both pure Bi and some of its alloys with Sb at a field of 0.75 T.[29] The Seebeck coefficient of these alloys, as well as the magnetoresistance, increases with the length-to-width ratio in the presence of a magnetic field, indicating that the thermoelectric figure of merit in the presence of a magnetic field is very dependent on the structure of the composite.

The mechanical properties of sintered materials are generally superior to those of samples cut from melt-grown ingots. Here we discuss a route to the synthesis of materials which can result in improved thermal and electric properties. Our approach is to tailor the structure of the thermoelectric material on a micrometer and nanometer scale so that the combination of the relevant parameters result in an improved Z with respect to the bulk phase. The benefits, in both function and performance, from the development of synthetic systems with hierarchical structure is well known.[30] The interest in low dimensional thermoelectric materials has been stimulated by suggestions that one- and two-dimensional systems would give a greatly enhanced figure of merit.[31,32,33] Realization of this potential, which is limited by processing technology and cost, is facilitated by recent advances in nanocomposite fabrication and in related analytical tools such a scanning electron and atomic force microscopies. Other interesting materials in the context of thermoelectricity are superlattices, which are reviewed elsewhere.[34] Here we emphasize recent work on wire arrays. This type of composite is made by

injecting porous materials with a conducting phase. By utilizing microchannel and nanochannel insulators as hosts or template structures, we benefit from increasing momentum in the technology of microporous dielectrics,[35,36].

It has been suggested that microengineering traditional thermoelectric materials into composites may lead to a significant improvement of their thermoelectric performance because of the reduction of phonon thermal conductivity from phonon scattering at the grain boundaries and interfaces. Furthermore, the composite figure of merit ZT may be dramatically increased over that for bulk because of the increase of the electronic density of states that occurs in low dimensionality systems. We have prepared oriented Bi_2Te_3 nanowire arrays in porous alumina as well as random networks of Bi_2Te_3 nanocrystals. The trigonal Bi_2Te_3 crystallites that form the wires are oriented with the basal plane of the hexagonal cell, i.e., the plane of highest conductivity, along the wire length. Bi wire arrays are similarly oriented. This structural effect is a direct result of the high-pressure high-temperature processing. An implication of our results is that wire arrays have a higher figure of merit than the random networks.

Two types of Bi_2Te_3 composites were examined, namely wire arrays of oriented crystallites and semiconductor random networks in porous silica. The nanochannel alumina samples were injected with the Bi_2Te_3 melt at 700 C and 60,000 psi. Fig. 6 shows an electron micrograph of the composite.

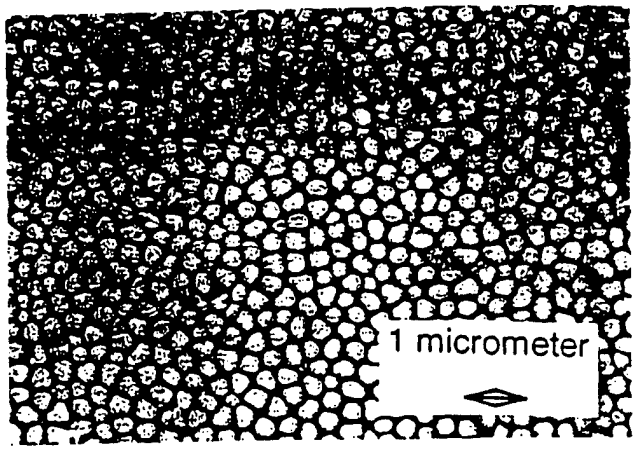

Fig. 6. SEM of a Bi_2Te_3 wire array composite (top view).

The nanowires grow with a preferred crystallographic orientation relative to their length. This is illustrated in the X-ray diffraction (XRD) spectrum of Fig. 7. The XRD spectrum is dominated by diffraction peaks from crystal planes parallel to the hexagonal c-axis. The trigonal bismuth telluride crystallites that form the wire are preferentially oriented with the basal plane of the hexagonal cell, i.e., the plane of highest conductivity, along the wire length (the c-axis perpendicular to the wire length).

An estimate for the average semiconductor crystallite size D can be obtained from the widths of the XRD peaks through Scherrer's equation.[37] A value of D= 40 nm is determined from the width of the peak at $2\theta = 41.5^{\circ}$ from the (110) plane, which is 0.24°. Figure 8 illustrates this configuration.

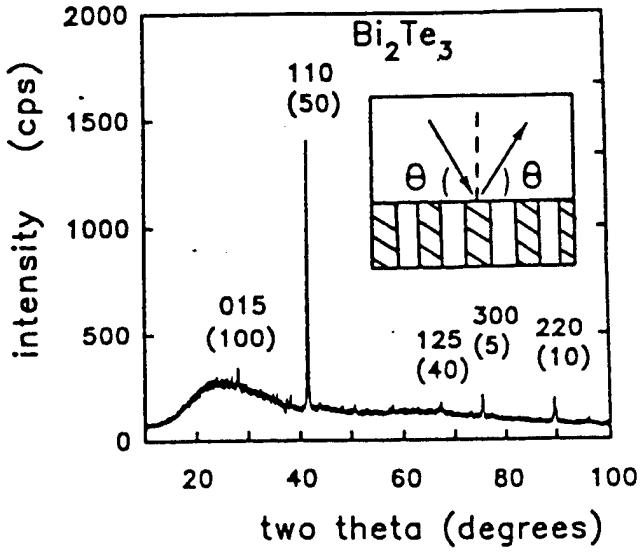

Fig. 7. X-Ray diffraction of a Bi_2Te_3 wire array composite. The inset shows the scattering geometry. The numbers in parenthesis indicate the relative intensities for random crystallites.

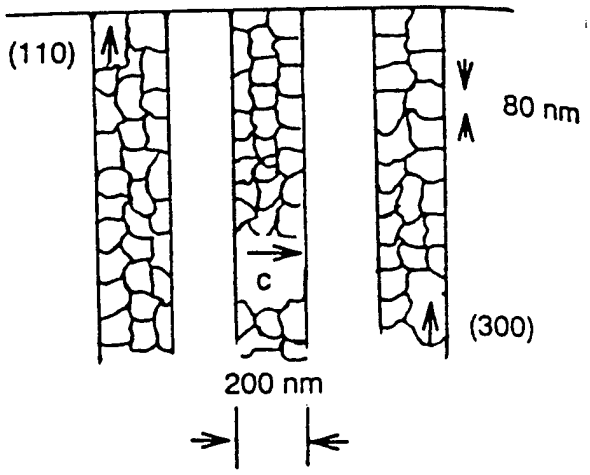

Fig. 8. Illustration of the crystalline structure of the Bi_2Te_3 wire array.

The orientation and size of the microcrystals forming the wires is determined during the nucleation

process, where nuclei grow by adding single atoms to the growing cluster of atoms having the configuration of the solid. This may happen homogeneously somewhere in the volume of the melt or heterogeneously on the surface of the template. Since the surface area of the template is so large, the latter dominates. The existence of many nuclei may explain the small crystallite size. The clear predominance of Bi_2Te_3 crystallites oriented with the hexagonal c-axis perpendicular to the template surface likely results from the weaker, and thus easier to break, bonds along that axis.

We have also prepared and examined nanocomposites where the conducting phase is injected in porous Vycor glass (PVG). The Vycor glass used in this study has an average pore diameter of 5.6 nm as determined through nitrogen adsorption/desorption measurements. The interconnected porous network has a volume of roughly 32% of the total sample volume. The Bi_2Te_3 fills approximately 95% of the pore volume. X-ray diffraction measurements show that the Bi_2Te_3 retains its trigonal structure and the broadening of the X-ray peaks yields a characteristic crystallite size of roughly 30 nm, significantly larger than the pore size. This phenomenon has been observed in other composites of metals in porous Vycor glass.[38,39] The Seebeck coefficient of this composite is smaller than that of the bulk. The Seebeck coefficient is strongly dependent on the concentration of donor and acceptor impurities. The concentration of impurities can change during processing; a similar phenomenon has been observed in powder metallurgy of bismuth telluride. Quantum effects are unlikely to play a role here since the 6 nm pore size is larger than the sizes for which quantum confinement effects are expected to become significant for bismuth telluride.

Even if the concentration of impurities can be restituted to its optimal value, it is not difficult to show that the random network of Bi_2Te_3 has a low figure of merit. Since at room temperature the average phonon wavelength and mean free path are shorter than the pore diameter, the composite thermal conductivity is simply the sum of the contributions from the PVG matrix and the Bi_2Te_3 in the pores. Therefore, the composite thermal conductivity can be estimated from the expression $\kappa = (1-\phi)\,\kappa_{Silica} + \phi\,\kappa_{Bismuth\ Telluride}$, where ϕ is the volume fraction of the semiconductor or porosity, κ_{Silica} and $\kappa_{Bismuth\ Telluride}$ are the thermal conductivities of silica and bismuth telluride, respectively. The electrical conductivity of the Bi_2Te_3-SiO_2 composite, σ_c, can be obtained from the empirical expression describing the conductivity of a porous system saturated with a conducting fluid,[36] $\sigma_c = \sigma_b\,\phi^m$, where σ_b is the conductivity of bulk Bi_2Te_3 and m is roughly 2. Accordingly, the electrical conductivity is reduced roughly by a factor of ten in the random network composite. Results of these estimates are shown in Table I. In estimating the figure of merit in Table I we have neglected the electronic contribution to the thermal conductivity. The electronic contribution to the thermal conductivity in the

bulk is approximately κ_e = 0.3 mW/cm.K at room temperature, much less than the lattice thermal conductivity κ_L = 1.5 mW/cm.K.

To estimate the properties of wire arrays we have assumed that the matrix is silica glass, such as microchannel plates and the recently developed nanochannel glass. (In fact, we have used Anopore in our experiments. Anopore is basically porous alumina and has a higher thermal conductivity than silica glass). This allows for comparison of geometrical effects in the two composites. Table I shows that the random networks have a considerably lower figure of merit than the bulk material and the wire arrays. The wire arrays suffer a 50% "geometrical" degradation in the figure of merit. This effect can be minimized using higher porosity matrices. For example, for microchannel plates, the reduction of the figure of merit is estimated to be only 25%.

	bulk Bi_2Te_3 [1] (off-the shelf)	Bi_2Te_3- SiO_2 networks (6 nm diameter) (ϕ = 0.32)	Bi_2Te_3 wire array (200 nm diameter) (ϕ = 0.5)
S(μV/K)	230	164[2]	230[3]
σ (Ω^{-1}.cm^{-1})	500	50[4]	250[4]
κ (mW.cm^{-1}.K^{-1})	16	14[4]	12.3[4]
Z T (T= 300 K)	0.5	0.06	0.32

Table I. Thermoelectric properties of bismuth telluride composites. S is the Seebeck coefficient, and σ is the electrical conductivity. The thermal conductivities are defined in the text.

(1) Properties of the undoped material at 20 °C, from Ref. 27.

(2) Measured.

(3) For comparison purposes, assumed to be the same as in column 1.

(4) Estimated

Casual inspection of Table I suggests that the performance of the composites may be inferior than that of the bulk thermoelectric phases. The thermoelectric figure of merit of composites has also been addressed by D.J. Bergman.[41] His conclusion is that by mixing together microscopically a number of difference thermoelectric components, the figure of merit can never be greater than the largest amongst the various component values. We discuss this point further in Section 3, Proposed Research.

2.4 Electronic Transport in a Bismuth Nanowire Network

It is well known that Bi has a large thermoelectric figure of merit at intermediate temperatures at around 100 K in the presence of a magnetic field B ~ 1 T. Bismuth is a semimetal whose three-conduction band minima at the L-points overlap the valence-band maximum at the T-point by about 40 meV. The electron effective mass along certain axes is very small and therefore quantum confinement effects can be very large. Lutskii[42] and Sandomirskii[43] pointed out the possibility of a SMSC transition to occur when the energy shift due to confinement becomes large enough to raise the lowest electron sub-band to an energy higher than that of the uppermost hole subband. This would make Bi even more desirable because semiconductors are typically better thermoelectric materials than semimetals. For thin films the critical thickness t_c for this transition is expected to be 30 nm. Despite many transport and optical investigations of quantum phenomena in (two-dimensional) thin films the experimental evidence is not conclusive. Those films exhibit a high resistivity ρ and a weak temperature dependence of ρ, unlike a typical intrinsic semiconductor. This has been interpreted in terms of a very short effective mean free path $l \sim t$, where t is the film thickness, and an enhanced semiconductor carrier density.[44] The alternative view, that the SMSC does not occur for disordered boundaries, also has proponents.[45]

Confinement introduces scattering and it is known that electronic transport in disordered conductors can occur in ballistic, diffusive (resistive) or localized regimes. It has also been found that many metallic systems of restricted geometry (wires and films) appear to have $d\rho/dT < 0$ at low enough temperatures, suggesting that they are in effect insulators ($\rho = \infty$ for T=0). A localization correction to the resistance appears because the elastic lifetime of an electron τ_e in an eigenstate of momentum is much smaller that the inelastic lifetime of an eigenstate of energy τ_ϕ. As a consequence, a charged carrier in a state of momentum K can be scattered by the interfaces without losing its phase coherence. The resistance rise can be expressed as $\delta R/R \approx \Lambda/L_q$, where L_q is the length of a conductor having the characteristic quantum resistance $4h/e^2 \approx 16.4\ k\Omega$, that is $L_q = (A/\rho)(4h/e^2)$ with A the cross-sectional

area. Λ is a function of the inelastic scattering times and has been derived in the localization[46] and interaction[47] models. The length Λ has a different meaning in the two models. The application of these ideas to metallic[48] and Bi[49] thin 2-dimensional and 3-dimensional films is well known. Bi, being a heavier metal, has a large spin-orbit interaction which may complicate the analysis of the magnetoresistance. Recently, fairly detailed models of the conductance and of other transport properties such as thermopower[33,50] have been developed for Bi quantum wires. Experiments lag behind. We have recently presented the first experimental investigation of the temperature T and magnetic-field B dependent resistivity ρ of networks of wires of diameter d=6 nm. Since this is much smaller than the critical diameter for the SMSC transition we expect that this type of experiments will help clarify this matter.[51]

The samples are prepared by melting pure Bi (99.9999 %) and injecting it into porous Vycor glass (PVG) by applying hydrostatic pressures of a few kilobars. The PVG used has an average pore diameter *d* of 6 nm. The interconnected network of pores occupies approximately 30% of the total volume. While the silica backbone structure is complex and interconnected, one can consider it as being made up of silica particles of a characteristic size of 26 nm. SAXS measurements of selenium-filled Vycor samples show that the host matrix structure is unchanged by the injection process, and we assume that the same is true for the Bi-injected samples. X-ray diffraction (XRD) measurements on the composite show that Bi retains its rhombohedral (trigonal) structure but with a considerable shrinkage of the unit cell parameters. Fig. 9 shows the resistance as a function of temperature. The resistivity of Bi-injected Vycor exhibits a non-metallic temperature dependence. The temperature dependence observed is approximated by ln(1/T) at low temperatures. The network of nanowires fails to display the temperature-activated behaviour of an intrinsic semiconductor. At intermediate temperatures between room temperature and 4 K the confined Bi resistivity displays the behaviour expected for a non-intrinsic semiconductor in the presence of interfacial states. Our observations suggest a concentration of surface states of 5×10^{18} /cm^3. This temperature dependence of the resistivity is typical of a disordered system and it shows many similarities with Bi thin films.[44]

The nature of electron transport is relevant to thermoelectrics properties since quantum efffects are only trully anticipated for ballistic transport. The observed temperature rise at low temperatures is interpreted in terms of weak localization effects due to disorder, in complete analogy to thin films. These effects are characteristic of the ballistic regime where l_ϕ the dephasing mean free path, is larger than the elastic mean free path l_e. Localization effects can be examined through the magnetic field dependence of the resistance; the magnetic field suppresses the temperature dependence of the weak

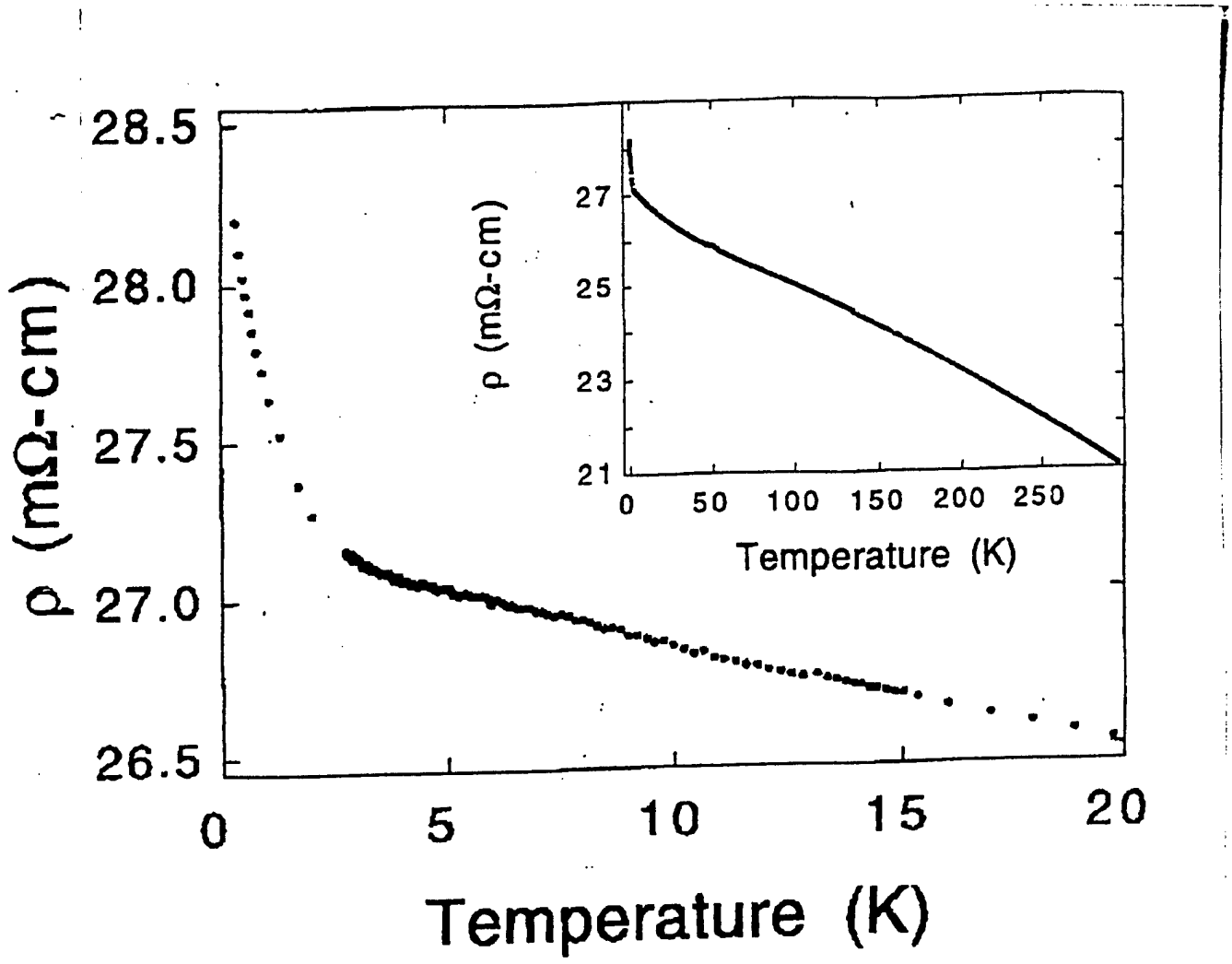

Fig. 9. Low temperature resistivity of Bi-injected PVG. Inset: The resistivity over the room-temperature to 0.3 K range.

localization and only the Coulomb anomaly remains. By examining the magnetoresistance[47,48] and under the assumption assuming that the material is composed of 6 nm diameter wires, values for l_ϕ and for l_{so} the dephasing time from spin-orbit coupling. Thus, best fit to the 2.3K magnetoresistance data is obtained for l_ϕ = 1000 nm and l_{so} = 400 nm. These values satisfy the condition that $l_{so}, l_\phi >> l_e \sim d$ for ballistic transport at T < 4 K.[52] More detailed studies are needed to evaluate l_{so} and l_ϕ at intermediate temperatures around 100 K.

Recently, Z. Zhang, J.Y. Ying, and M.S. Dresselhaus have reported on the fabrication of Bi wire arrays in anodic alumina with wire diameters ranging between 56 nm and 13 nm.[53] They describe a synthetic route identical to the pressure injection utilized in our research. They do not present direct transport measurements but instead optical absorption spectra of the nanowire arrays. Their room-temperature data show an increase in absorption for high frequencies for the 13 nm and 23 nm diameter wires. Instead, the 56 nm diameter wire shows opposite behaviour. The authors suggest that these changes are brought about by a change in the band-gap energy of the Bi nanowires as a function of wire diameter. This in turn suggests a bismuth nanowires semimetal-to-semiconductor transition in the Bi nanowire. We believe this evidence to be indirect and insufficient. Furthermore, it is surprising that the near-infrared absorption reported for the small diameter wires is so small, considering that the energy band of the confined Bi would be rather small (tens of meV)

BIBLIOGRAPHY

1. An overview can be found in the *Proceedings of the First International Conference on Nanostructured Materials*, Cancun, 1992, M.J. Yacaman, T. Tsakalakos, and B.H. Kear, eds., *Nanostructured Materials* **3** (1993).
2. Rustum Roy, *Nanophase and Nanocomposite Materials*, S. Komarneni, J.C. Parker, and G.J. Thomas, eds, *Mat. Res. Soc. Symp. Proc.* **286**, 241 (Materials Research Society, Pittsburgh, 1993), and references therein.
3. N.F. Borrelli and J.C. Luong, *Materials and Technologies for Optical Communications*, Cannes, 1987, *Proc. SPIE-Int. Soc. Opt. Eng.* **866**, 104 (1988).
4. B.L. Justus, R.J. Tonucci, and A.D. Berry, *Appl. Phys. Lett.* **61**, 3151 (1992).
5. M.J. Tierney and C.R. Martin, *J. Phys. Chem.* **93**, 2878 (1989).
6. G.D. Stucky and J.E. Mac Dougall, *Science* **247**, 669 (1990) and references therein.
7. P.M. Ajayan and S. Iijima, *Nature* **361**, 333 (1993).
8. R.J. Tonucci, B.L. Justus, A.J. Campillo, and C.E. Ford, *Science* **258**, 783 (1992).
9. C.T. Kresge, M.E. Leonowicz, W.J. Roth, J.C. Vartuli, and J.S. Beck, *Nature* **359**, 710 (1992).
10. C.A. Huber and T.E. Huber, *J. Appl. Phys.* **64**, 6588 (1988).
11. T.H. Elmer, I.D. Chapman, and M.E. Nordberg, *J. Phys. Chem.* **66**, 1517 (1962).
12. D. Chacko-Davis, M.S. Thesis at Howard University (1996), and D. Chacko-Davis and T.E. Huber, to be published.
13. For a review, see Y. Yablonovitch, *J. Opt. Soc. Am.* **B10**, 283 (1993).
14. J.B. Pendry, A.J. Holden, and W.J. Stewart, *Phys. Rev. Lett.* **76**, 4773 (1996).
15. F. Zhou, B. Spivak, N. Taniguchi, and B.L. Altshuler, *Phys. Rev. Lett.* 77, 1958 (1996).
16. D.E. Aspnes, A. Heller, and J.D. Porter, *J. Appl. Phys.* **60**, 3028 (1986)
17. G. Brändli and A.J. Sievers, *Phys. Rev.* **B5**,2550 (1975).
18. A. Heller, D.E. Aspnes, J.D. Porter, T.T. Sheng, and R. G. Vadimsky, *J. Phys. Chem.* **89**, 4444 (1985).
19. M.J. Tierney and C. R. Martin, *J. Phys. Chem.* **93**, 2878 (1989).
20. C.A. Foss, G.L. Hornyak, J.A. Stockert, and C. R. Martin, *J. Phys. Chem.* **98**, 2963 (1994).
21. T.E. Huber and L. Luo, *Appl. Phys. Lett.* **98**, 2502 (1997).
22. T.E. Huber, L. Silber, and F. Boccuzzi, Phys. Rev. 1998.
23. Tito E. Huber, Laura Luo, Frank Boccuzzi, and Leo Silber, Optical Materials **9**, 373 (1997).
24. R.E. Collin in *Field Theory of Guided Waves* (McGraw-Hill, New York, 1960, Ch. 12).

25. S.B. Cohn in *Modern Advances in Microwaves Techniques*, Polytechnic Institute of Brooklyn Symposium Proc. Vol 4, p. 465, edited by E Cassedy, Jr.
26. T.E. Huber and Leo Silber, Symposium on Low Dielectric Constant Materials for Microelectronics (Materials Research Society, San Francisco, 1998).
27. H.J. Goldsmid in *Electronic Refrigeration*, 2nd edition (Pion Limited, London, 1986).
28. W.M. Yim and A. Amith, *Solid-State Electronics* **15**,1141 (1972).
29. M.E. Ertl, G.R. Pfister, and H.J. Goldsmid, *Br.J. Appl. Phys.* **14**,161 (1963).
30. Committee on Synthetic Hierarchical Structures, National Research Council, NMAB-464 (National Academic Press, Washington, D.C. 1994).
31. L.D. Hicks and M. Dresselhaus, *Phys. Rev.* **B47**, 12727 (1993).
32. L.D. Hicks, T.C. Harman, and M.S. Dresselhaus, *Appl. Phys. Letters* **63**,3230 (1993).
33. L.D. Hicks and M.S. Dresselhaus, *Phys. Rev.* **B47**, 16631 (1993).
34. T.L. Reineke and D.A. Broido, *Phys. Rev.* **B51**, 13797 (1995).
35. One indication of growing interest on microporous templates is the large number of companies listed in the 1998 Physics Today Buyers's Guide under the classification of microchannel array plates.
36. C.A. Huber, T.E. Huber, M. Sadoqi, J.A. Lubin, S. Manalis, and C.B. Prater, *Science* **263,** 800 (1994)
37. H.P. Klug and L.E. Alexander, *X-Ray diffraction Procedures for Polycrystalline and Amorphous Materials* (J.W. Wiley and Sons, 2nd edition, New York, 1974).
38. W.H. Yang, T.E. Huber, J.A. Lubin, G.E. Walrafen and C.A. Huber, in "Nanophase and Nanocomposite Materials", S. Komarnierni, J.C. Parker and G.J. Thomas, Eds. Mat. Res. Symp. Proc. **286**, 419 (1993).
39. C.A. Huber, M. Sadoqi, and T.E. Huber, *Advanced Materials* 7, 316 (1995).
40. T.E. Huber and R. Calcao, Proc of the 1997 International Conference on Thermoelectrics, edited by A. Heinrich (IEEE, 1997), pp. 404.
41. D.J. Bergman, Proc. Of the 1997 International conference on Thermoelectrics edited by A. Heinrich (IEEE, 1997), pp. 401.
42. V.N. Lutskii, *JETP Lett.* **2**, 245 (1965).
43. V.B. Sandormirskii, *JEPT* **25**, 101 (1967).
44. C.A. Hoffman, J.R. Meyer, F.J. Bartoli, A. Di Venere, X.J. Yi, C.L. Hou, H.C. Wang, J.B. Ketterson, and C. K. Wong, *Phys. Rev.* **B48**, 11431 (1993).
45. H.T. Chu, P.N. Henriksen, and J. Alexander, *Phys. Rev.* **B37**, 3900 (1988).
46. D.J. Thouless, *Phys. Rev. Lett.* **39**, 1167 (1977); P.W. Anderson, D.J. Thouless,

E. Abrahams, and D.S. Fisher, *Phys. Rev.* **B22**, 3519 (1980).

47. B.L. Altshuler, D. Khmel'nitzkii, A.I. Larkin, and P.A. Lee *Phys. Rev.* **B22**, 5142 (1980).

48. Y. Imry in *Introduction to Mesoscopic Physics* (Oxford University Press, Oxford, 1997).

49. Y.F. Komnik, E.I. Bukhshtab, and Y.V. Nikitin, Sov. *J. Low. Temp. Phys.* 7, 656 (1982). Y.F. Kommik, E.I. Bukhshtab, A.V. Butenko, and V.V. Andrievsky, *Solid State Comm.*, **44**, 865 (1982).

50. E.N. Bogacheck, A.G. Scherbakov, and U. Landman, in *Nanowires*, edited by P.A. Serena and N. Garcia (Kluwer, Dordrecht, 1997).

51. T.E. Huber and M.J. Graf, Phys. **B60** Rev. Dec 1999

52. However, since our wires are short, $l_{e.e.}, l_\phi >> l$ = 30 nm, use of the 1D expression is not completely justified and the magnetoresistance is also affected by the network structure. Wire networks are more complex than single wires and, in fact, in the length scale of l_ϕ the composite structure is probably 3-D. We discuss these issues in Ref. 51.

53. Z. Zhang, J.Y. Ying, and M.S. Dresselhaus, J. Mater. Res. **13** 1745 (1998).